

Modelocking of a GaInNAs VECSEL using a GaInNAs SESAM for 1.3 μm applications

Paolo Navaretti (1), Andreas Rutz (1), Valeria Liverini (1), Deran J. H. C. Maas (1), Benjamin Rudin (1), Aude-Reine Bellancourt (1), Silke Schön (2) and Ursula Keller (1)

1) ETH Zurich, Physics Department, Institute of Quantum Electronics
Wolfgang-Pauli-Strasse 16, CH-8093 Zürich, Switzerland
2) ETH Zurich, FIRST Center for Micro- and Nanoscience
Wolfgang-Pauli-Strasse 10, CH-8093 Zürich, Switzerland

Abstract: *In this paper we report the results of the first GaInNAs Vertical External Cavity Surface Emitting Laser (VECSEL) modelocked using a GaInNAs Semiconductor Saturable Absorber Mirror (SESAM). The intracavity SESAM provides self-starting of stable modelocking for the optically-pumped VECSEL. Trains of pulses 18.6 ps long with a repetition rate of 6.1 GHz and an average power of 57 mW were obtained at 1308 nm using this system. Operating the VECSEL in continuous-wave (cw) regime we obtained an average output power of 560 mW in single TEM₀₀ mode.*

Introduction

Broadband high-speed optical networks require stable short-pulse sources with high repetition rates operating at an optical wavelength of 1.3 μm , where the zero-dispersion in silica fibers occurs.

Passive modelocked VECSELs provide stable pulse trains in the picosecond and sub-picosecond regime with multi-GHz repetition rates and power scaling up to a few watts for optical pumping [1].

Emission in the 1.3- μm wavelength range can be obtained using GaInNAs quantum well (QW) systems, which, in the last few years, proved to be excellent candidates for the active region in laser diodes [2].

Optically pumped VECSELs have been modelocked for the first time in 2000 [3]. Since then the research efforts in this field made it possible to obtain higher repetition rates [4], higher average output power [5] and different wavelengths. However, previously no VECSEL has been modelocked at the wavelength of 1.3 μm .

Before this result, GaInNAs SESAMs were used to modelock solid-state lasers both at 1.3 [6] and at 1.5 μm [7]. Here we report on the modelocking of a GaInNAs VECSEL using a GaInNAs SESAM.

In order to use the same material for both the gain and absorbing media different growth and processing procedures must be applied in order to optimize the material characteristics to the application. Indeed, GaInNAs is very susceptible to different growth and processing conditions, dramatically changing optical properties on slight changes of one of the parameters of its production process. This characteristic, alongside with the lattice compatibility to GaAs and the large wavelength tunability with nitrogen concentra-

tion, makes this compound semiconductor an ideal candidate for passive modelocking in the 1.3 μm wavelength range.

Since GaInNAs has been proposed by Kondow and co-workers [8] as the gain material for telecommunication lasers, its optical quality has improved substantially. However the optical efficiency is still affected by growth time incorporation of nonradiative defects that have to be cured post-growth with the use of thermal treatments [9].

These non-radiative defects can, on the other hand, be exploited to make saturable absorbers with fast recovery characteristics.

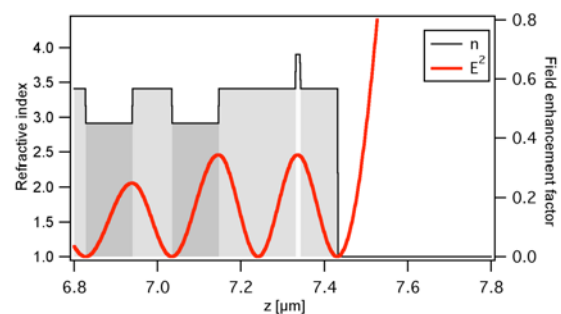


Fig. 1 SESAM design: refractive index (left axis) and electric field enhancement factor (right axis) in the top 0.6 μm of the SESAM device.

Growth and processing of the SESAM and the VECSEL structures

The SESAM structure has been grown entirely by molecular beam epitaxy (MBE) on an undoped (001) GaAs substrate. It consists of a 35-pair AlAs/GaAs distributed Bragg reflector (DBR) centered at 1310 nm, a 90 nm GaAs spacer layer, a 10 nm Ga_{0.65}In_{0.35}N_{0.016}As_{0.984} absorber and finally a 90 nm GaAs cap. This last layer has the function of making the structure antiresonant, thus giving it negligible group delay dispersion at the wavelength at which it is centered [10]. The refractive index and field enhancement factor versus device thickness is shown in figure 1. The indium and nitrogen concentrations were chosen such that the photoluminescence (PL) wavelength occurs around 1310 nm. Since the PL emission wavelength corresponds to the onset of absorption, this choice placed the absorption edge very close to the laser wavelength, thus giving the SESAM low saturation fluence in our laser setup

[11]. The absorption spectrum of this SESAM is plotted in figure 2.

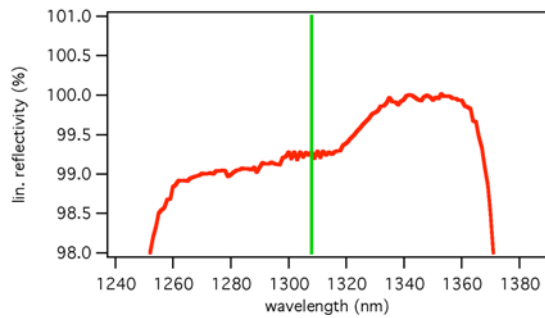


Fig. 2 Reflectivity spectrum of the SESAM. The vertical line indicates the laser wavelength.

No post growth processing was applied to the SESAM.

The VECSEL structure was grown upside-down in order to be able to subsequently remove the substrate from the device for better heat removal during operation [12]. At first an etch stop structure was grown on an undoped (001) GaAs substrate. It consisted of three layers of different materials: $\text{Al}_{0.85}\text{Ga}_{0.15}\text{As}$, GaAs and AlAs. On top of the etch-stop, an antireflection (AR) structure was grown to minimize reflection losses from the VECSEL surface of both the pump wavelength at 45° of incidence and of the laser wavelength normal to the surface. This structure consists of 10 layers of AlAs and $\text{Al}_{0.20}\text{Ga}_{0.80}\text{As}$. Their thicknesses were numerically optimized for an antireflection effect for both wavelengths. The choice of $\text{Al}_{0.20}\text{Ga}_{0.80}\text{As}$ instead of pure GaAs in the DBRs of the VECSEL is to minimize the absorption of the pump outside of the gain region.

After the AR structure, the active region has been grown. This consists of 5 $\text{Ga}_{0.65}\text{In}_{0.35}\text{N}_{0.018}\text{As}_{0.982}$ quantum wells (QWs) 8 nm thick. We designed the QWs each at different antinode of the standing wave of the laser electric field and, therefore, designed the GaAs barriers separating them to be 178 nm thick.

The growth of these structures has been conducted using the same MBE used for the the growth of the SESAM. The DBRs of the VECSEL were, instead, grown by metal-organic vapor phase epitaxy (MOVPE). The laser mirror consists of 32 pairs of AlAs/ $\text{Al}_{0.20}\text{Ga}_{0.80}\text{As}$ whose thicknesses were chosen to give high reflectivity at 1300 nm under normal incidence. The pump DBR consists of 10 pairs of the same materials designed to reflect at 808 nm under an incidence angle of 45° . The refractive index and field enhancement factor versus device thickness of the top layers after substrate removal are shown in figure 3.

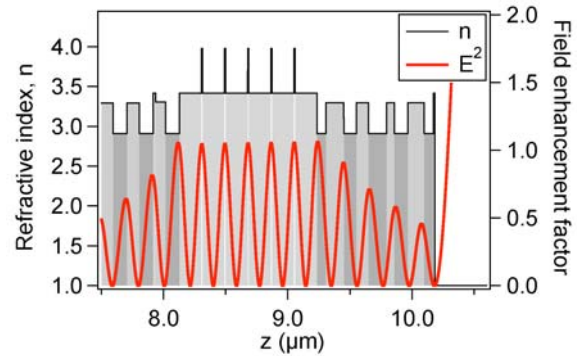


Fig. 3 VECSEL design: refractive index (left axis) and electric field enhancement factor (right axis) as a function of distance in the top 3 μm of the VECSEL device.

Two main characteristics distinguish the GaInNAs material used in the active structure from the one used in the absorber: a slight difference in nitrogen composition and a different growth temperature. The slightly higher nitrogen concentration in the gain material is necessary to compensate for the thermal treatment due to the high-temperature growth of the DBR. This improves the optical quality but also blueshifts the optical emission [13][14]. More nitrogen is, therefore, necessary to obtain lasing at 1300 nm.

The difference in growth temperature is due to the fact that GaInNAs has a higher optical efficiency when grown at lower temperatures and then annealed. These low temperatures, on the other hand, tend to make its recovery time longer. For this reason the active region material has been grown at a lower temperature of 410°C than the one of the absorbing material, which was of 450°C .

After growth was completed the VECSEL required further processing steps before it could be used in the laser. First, the surface was metallized with indium and soldered face-down in vacuum to a copper heat sink. Afterwards, the substrate was removed by a combination of mechanical lapping and wet chemical etching. The final surface was etch-pit free and mirror-like, denoting very high quality of the growth and of all the processing steps involved in its preparation.

Characterization of the SESAM and of the VECSEL

The SESAM has been characterized by pump-probe and nonlinear reflectivity techniques in order to assess its recovery time and nonlinear absorption characteristics [15]. This resulted in a low saturation fluence of 6.8 (± 0.2) $\mu\text{J}/\text{cm}^2$, a low modulation depth of 0.76%, nonsaturable losses of 0.12% and a recovery time of about 47 ps, which is suitable for modelocking in the ps-pulse regime [16].

Laser setup and cw results

The cw lasing characteristics of the VECSEL were tested using a similar cavity as for modelocking, simply replacing the SESAM with a high reflectivity DBR mirror. We used an 808 nm free-space diode laser as the pump and a 1.5% output coupler with a radius of curvature of 100 mm. With this configuration we obtained 560 mW of output power in single TEM₀₀ mode at a wavelength of 1280 nm.

For modelocking, the laser was built as a V-cavity configuration, with on one arm of the V a 0.7% transmission output coupler with a radius of curvature of 25 mm and on the other one the SESAM (substituted by a DBR in the cw measurements). The VECSEL was positioned at the intersection of the arms. The 808 nm free-space diode laser provided the pump power and was positioned so that it hit the VECSEL under an angle of 45° [17].

The SESAM was placed 8 mm from the VECSEL and the output coupler at approximately 16 mm for a total cavity length of 24 mm. A 25 μm fused silica etalon was inserted between the VECSEL and the output coupler to provide wavelength stabilization. The VECSEL stage was cooled to 5°C using peltier elements.

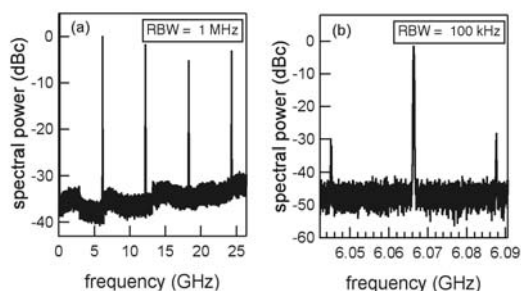


Fig. 4 Microwave spectra: (left) 25 GHz span with a resolution bandwidth of 1 MHz, (right) 50 MHz span with a resolution bandwidth of 100 kHz, centered around the main peak.

Modelocking results

We obtained stable self-starting cw modelocking with a repetition rate of 6.1 GHz. Figure 4 (left) shows the microwave spectrum of the laser with a full span from DC up to 25 GHz. Figure 4 (right) shows the same spectrum but centered to the pulse repetition rate and with a span of only 50 MHz. From the latter it is possible to notice two side peaks around the main peak separated by about 20 MHz from it. These are suppressed by more than 30 dB and we believe they might be due to higher-order mode beating as the cavity length influences their separation from the main peak.

Figure 5 shows the autocorrelation signal of the pulse train generated by our modelocked VECSEL. This has been fitted using a sech^2 function and a pulse duration of 18.6 ps was obtained. Figure 6 shows the optical spectrum collected using a 0.1 nm spectrum analyzer.

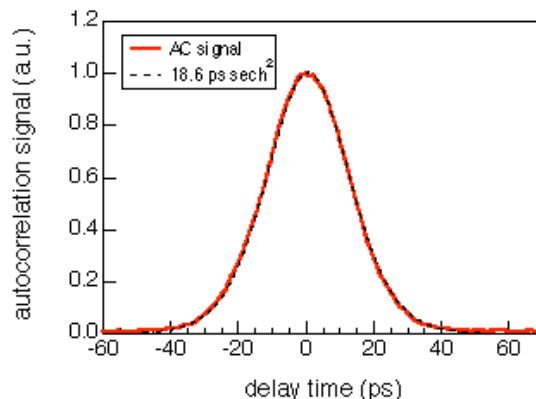


Fig. 5 Autocorrelation signal fitted to a sech^2 function.

The average power obtained in the modelocked regime was 57 mW under a pump power of 3 W.

Measurements of the beam profile using a knife-edge beam profiling system yielded an M^2 value of 1.15, which supports the theory of higher-mode beating to explain the side peaks.

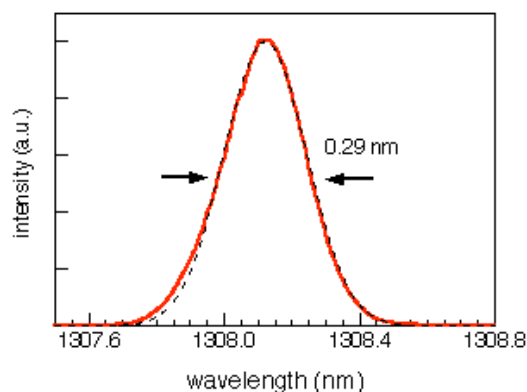


Fig. 6 Optical spectrum of the modelocked VECSEL fitted to a gaussian function.

Conclusions

We have reported the results of the first 1.3 μm VECSEL modelocking. This result has been obtained using GaInNAs in the dilute nitrogen regime for both the gain and absorbing media. Self-starting modelocking with pulses in the picosecond regime and repetition rates in the GHz range have been demonstrated.

Acknowledgments

We wish to acknowledge NCCR for funding this project under the Quantum Photonics framework. We also thank Dr. Emilio Gini for the MOVPE growth.

References

- 1 U. Keller et al., Physics Reports 429 (2) , p. 67, 2006.
- 2 N. Tansu et al., Appl. Phys. Lett. 83, p. 18, 2003.

- 3 S. Hoogland et al., IEEE Photon. Technol. Lett. 12, p. 1135, 2000.
- 4 D. Lorenser et al., Appl. Phys. B 79, p. 927, 2004.
- 5 A. Aschwanden et al., Opt. Lett. 30, p. 272, 2005.
- 6 V. Liverini et al., Appl. Phys. Lett. 84, p. 4002, 2004.
- 7 A. Rutz et al., Elec. Lett. 41, p. 321, 2005
- 8 M. Kondow et al., Jpn. J. Appl. Phys., Part 1 **35**, p.1273, 1996 .
- 9 M. Kondow et al, Journal of Physics: Condensed Matter 16, p. S3229, 2004.
- 10 G. Spühler et al., Appl. Phys. B 81, p. 27, 2005.
- 11 R. Grange et al., Appl. Phys. Lett 87, p. 132103, 2005.
- 12 R. Häring et al, Electron. Lett. 37, p. 766, 2001.
- 13 V. Liverini et al., J. Appl. Phys. 99, p. 113103, 2006.
- 14 E.-M. Pavelescu, Appl. Phys. Lett. 83, p. 1497, 2003.
- 15 M. Haiml et al., Appl. Phys. B 79, p. 331, 2004.
- 16 R. Paschotta et al., Appl. Phys. B 73, p. 653, 2001.
- 17 A. Aschwanden et al., Appl. Phys. Lett. 86, p. 131102, 2005.